

**NATIONAL UNIVERSITY OF SCIENCE AND TECHNOLOGY
POLITEHNICA BUCHAREST**



Doctoral School of Chemical Engineering and Biotechnologies

Department of Science and Engineering of Oxide Materials and Nanomaterials

PhD Thesis

**NANOSTRUCTURED MATERIALS WITH
BIOMEDICAL APPLICATIONS**

- Resume -

PhD Supervisor

Prof. Dr. Eng. Cristina BUSUIOC

PhD Student

MSc. Eng. Andrada Elena ALECU
(NICOARĂ)

PhD committee

Committee president	Prof. Dr. Eng Ileana RĂU	From	National University of Science and Technology POLITEHNICA Bucharest
PhD Supervisor	Prof. Dr. Eng. Cristina BUSUIOC		
Member	Prof. Dr. Eng. Georgeta VOICU		
Member	CSI Dr. Eng. Monica ENCULESCU	From	National Research and Development Institute for Materials Physics
Member	Conf. Dr. Eng. Radu LAZĂU	From	University Politehnica Timișoara

BUCHAREST

2023

Contents

PART I - State of the Art

1. Introduction

2. Calcium magnesium silicates

2.1 Thermal phase diagram

2.2 Structure

2.3 Synthesis methods

2.4 Applications in medicine and other fields

3. Polymers used in tissue engineering

3.1 Types of polymers

3.2 Poly - ϵ - caprolactone (properties and biomedical applications)

3.3 Poly(vinylidene) fluoride (properties and biomedical applications)

4. Materials processing methods

4.1 Electrospinning method

4.2 Porogenic agent method

4.3 Sol-gel and precipitation methods

5. Composite materials based on polymers fibres and mineral phases

5.1 Combining electrospun fibres with bioactive phases

5.2 Combining electrospun fibres with antibacterial agents

PART II - Original contributions

General and specific objectives of the research

Article 1 – Synthesis of Calcium Magnesium Silicates

Article 2 – Composites based on Polycaprolactone and Calcium Magnesium Silicates

Article 3 – Synthesis of TiO₂ nanoparticles

Article 4 – PVDF fibres obtained by electrospinning method

Article 5 – Porous Forsterite Ceramics Scaffolds

General conclusions and originality

Results dissemination

References

List of figures

Part I - State of the Art

Fig. 1. Radiography of rabbits' tibia after the implantation (postoperative), 30 days after implantation, 60 days after implantation [31].

Fig. 2. SEM images of merwinite microstructures (a) before and (b) after 14 days of immersion in SBF [32].

Fig. 3. Congruent ternary diagram of the CaO-MgO-SiO₂ system at 1 bar pressure [58].

Fig. 4. Wollastonite - 3D crystal structure.

Fig. 5. Forsterite - 3D crystal structure.

Fig. 6. Diopside - 3D crystal structure.

Fig. 7. Akermanite - 3D crystal structure.

Fig. 8. Merwinite - 3D crystal structure.

Fig. 9. Silica content in various agricultural waste [80].

Fig. 10. SEM images of diopside surfaces sintered at 1100°C for 2 h (a) before and (b) after 3 days and (c) 7 days of immersion in SBF [82].

Fig. 11. Frequency usage of ceramic synthesis technology [93].

Fig. 12. Diopside scaffold with interconnected pores obtained by laser printing, different views: (a) above view, (b) lateral view, (c) overview [69].

Fig. 13. Apatite layer on diopside scaffold surface after different time of immersion in SBF: (a) after 14 days, (b) after 21 days, (c) after 28 days, (d) apatite layer at high magnification; and EDS spectra (e) before and (f) after diopside scaffold immersion in SBF [69].

Fig. 14. SEM images of akermanite scaffold obtained from Ak hydrated fillers (Mg(OH)₂ and hydrated borax) (a), (b) top view, (c), (d) section views [100].

Fig. 15. Synthetic polymers applications for targeted regenerated tissues [109].

Fig. 16. Potentially bioresorbable materials used for vascular scaffolds [118].

Fig. 17. Piezoelectric biodegradable materials and their medical applications [123].

Fig. 18. Potential use of electroactive materials in human body electrosensitive tissues [125].

Fig. 19. Electroactive materials applications [125].

Fig. 20. Structures made of PCL: nanospheres (a, b), nanofibres (c, d), foams (e, f), woven textiles (g, h, i), scaffolds selectively manufactured with laser (j-o). scaffolds modelled by melt deposition (p-u) [129].

Fig. 21. PVDF β -phase obtained from α and γ phases transition [138, 139].

Fig. 22. Usage of PVDF as biomaterial in medicine [142].

Fig. 23. Electrospinning equipment for a PVDF polymer solution [136].

Fig. 24. Fibres obtained by electrospinning method [150].

Fig. 25. Schematic fabrication process of bone scaffold starting from: (a) sucrose skeleton; (b) composite injected in sucrose skeleton, and (c) resulted scaffold after the sucrose was washed out using water [153].

Fig. 26. Sol-gel process stages [155].

Fig. 27. Precipitation process for obtaining hydroxyapatite nanoparticles [162].

Fig. 28. SEM images performed on ZnO nanoparticles obtained by (a) sol-gel and (b) precipitation [164].

Fig. 29. SEM images of: (a) simple PCL fibres, (b) PCL with 1% wt. diopside, (c) PCL with 3 wt% diopside and (d) PCL with 5 wt% diopside after immersion in SBF for 28 days [165].

Fig. 30. SEM images at 2 magnifications representing PVA/Chitosan/Akermanite scaffolds obtained by electrospinning method with different contain of akermanite powder: (a, b) 0.5 wt%, (c, d) 1 wt% and (e, f) 2 wt% [55].

Fig. 31. The percentage of articles based on electrospun fibres with various antibacterial nanoparticles [167].

Fig. 32. Antibacterial activity against *S. Aureus* and *E. Coli* of: (a, b) negative control, (c, d) simple ZnO particle, and Gelatin/ZnO fibres where concentration of ZnO particles suspension was: (e, f) 0%, (g, h) 0.1% and (i, j) 0.25% [168].

Fig. 33. Micrographs of live/dead bacterial test for *S. aureus* on mats: PVP (a), PVP-Ag (c), PVP-Cu (e), PVP-Zn (g) and for *E. coli* on mats: PVP (b), PVP-Ag (d), PVP-Cu (f), PVP-Zn (h) [170].

Fig. 34. The main materials obtained for the proposed objective.

Table 1. Cumulated impact factor

Part II - Original contributions

Article 1

Figure 1. Complex thermal analyses of the dry gels corresponding to: diopside (Dy), akermanite and merwinite (Mw) compositions. WL represents weight loss, DrTGA is the derivative thermogravimetric analysis and DTA stands for differential thermal analysis.

Figure 2. SEM images of the dry gels corresponding to: (a) diopside, (b) akermanite and (c) merwinite compositions.

Figure 3. SEM images of the ceramics corresponding to diopside composition, thermally treated at: (a,b) 600 °C; (c,d) 800 °C; and (e,f) 1000 °C.

Figure 4. SEM images of the ceramics corresponding to akermanite composition, thermally treated at: (a,b) 600 °C; (c,d) 1000 °C; and (e,f) 1300 °C.

Figure 5. SEM images of the ceramics corresponding to merwinite composition, thermally treated at: (a,b) 600 °C; (c,d) 1000 °C; and (e,f) 1300 °C.

Figure 6. EDX spectra of the dry gels and ceramics corresponding to: (a) diopside; (b) akermanite; and (c) merwinite compositions.

Figure 7. FTIR spectra of the dry gels and ceramics corresponding to: (a) diopside; (b) akermanite; and (c) merwinite compositions.

Figure 8. XRD patterns spectra of the dry gels and ceramics corresponding to: (a) diopside; (b) akermanite; and (c) merwinite compositions.

Table 1. Composition of the ceramics corresponding to diopside (Dy); akermanite (Ak); and merwinite (Mw) compositions, thermally treated at the highest temperature (1000 or 1300 °C).

Article 2

Table 1. Composition of the electrospinning solutions.

Figure 1. SEM images of the electrospun samples: (a,b) PCL, (c,d) PCL-D-5%, and (e,f) PCL-D-10%.

Figure 2. SEM images of the electrospun samples: (a,b) PCL-A-5%, (c,d) PCL-A-10%, (e,f) PCL-M-5%, and (g,h) PCL-M-10%.

Figure 3. EDX spectra of the electrospun samples with 5% powder loading.

Figure 4. FTIR spectra of the electrospun samples with 5% powder loading.

Figure 5. SEM images of the mineral powders after immersion in simulated body fluid for 4 weeks: (a) diopside, (b) akermanite, and (c) merwinite compositions.

Figure 6. Cell viability for fibroblasts in contact with the electrospun samples for 24 and 48 h.

Figure 7. Morphology of fibroblasts in contact with the electrospun samples for 24 h: (A) Control, (B) PCL, (C) PCL-D-5%, (D) PCL-D-10%, (E) PCL-A-5%, (F) PCL-A-10%, (G) PCL-M-5%, and (H) PCL-M-10%.

Article 3

Fig. 1. Thermal analyses of the dried precipitate and gel.

Fig. 2. (a) EDX and (b) FTIR spectra of the dried precipitate and gel, as well as powders calcined at 500 °C.

Fig. 3. (a) XRD patterns and (b) Raman spectra of the dried precipitate and gel, as well as powders calcined at 500 °C.

Fig. 4. SEM images of: (a) dried precipitate, (b) precipitate calcined at 500 °C, (c) dried gel and (d) gel calcined at 500 °C.

Fig. 5. (a) Reflectance spectra, (b) Kubelka-Munk functions and (c) PL spectra of TiO₂ powders.

Article 4

Table 1 Composition of the electrospinning solutions

Fig. 1 - SEM images of PVDF fibres obtained from:

PVDF-DMF-10 solution: (a) 0.2 mL/h, 20 cm, 15 kV, (b) 0.5 mL/h, 15 cm, 15 kV; PVDF-DMF-15 solution: (c) 0.4 mL/h, 20 cm, 15 kV, (d) 0.7 mL/h, 15 cm, 15 kV; PVDF-DMF-20 solution: (e) 0.5 mL/h, 20 cm, 15 kV, (f) 0.7 mL/h, 15 cm, 15 kV.

Fig. 2 - SEM images of PVDF fibres obtained from: (a and b) PVDF-DMF-DMSO-15 solution (0.2 mL/h, 20 cm, 15 kV); PVDF-DMF-1-Ac-1-15 solution: (c and d) 0.5 mL/h, 20 cm, 15 kV; (e and f) 0.7 mL/h, 15 cm, 15 kV.

Fig. 3 - SEM images of PVDF fibres obtained from PVDF-DMF-1-Ac-1-20 solution: (a and b) 0.5 mL/h, 20 cm, 15 kV; (c and d) 1.0 mL/h, 20 cm, 15 kV; (e and f) 1.0 mL/h, 20 cm, 18 kV.

Fig. 4 - SEM images of PVDF fibres obtained from PVDF-DMF-4-Ac-1-15 solution: (a and b) 0.5 mL/h, 20 cm, 15 kV; (c and d) 1.0 mL/h, 20 cm, 15 kV; (e and f) 1.0 mL/h, 20 cm, 18 kV.

Fig. 5 - SEM images of PVDF fibres obtained from PVDF-DMF-2-Ac-3-20 solution: (a and b) 0.5 mL/h, 20 cm, 15 kV; (c and d) 1.0 mL/h, 20 cm, 15 kV; (e and f) 1.0 mL/h, 20 cm, 18 kV.

Fig. 6 - SEM images of: (a and b) BT powder and (c-f) PVDF-BT fibres obtained from PVDF-DMF-2-Ac-3-20 solution with 3 wt% BT powder (1.0 mL/h, 20 cm, 18 kV). Images (c and d) are obtained using secondary electrons, while images (e and f) are obtained using back-scattered electrons.

Article 5

Table 1. Sample formulation and thermal conditions for obtaining ceramic materials.

Table 2. Chemical composition of samples after 14 days in SBF.

Figure 1. X-ray patterns of forsterite samples: untreated, F₁ and F₂.

Figure 2. X-ray patterns of forsterite samples: F₁20s and F₂20s.

Figure 3. SEM images magnification ×200 and ×20,000 of F₁ (a,b) and F₁20s (c,d) samples and pore dimension distribution (e); the pores are indicated with yellow arrows.

Figure 4. EDS spectra for: (a) F₁; (b) F₁20s samples.

Figure 5. SEM images magnification $\times 200$ and $\times 20,000$ of F₂ (a,b) and F₂20s (c,d) samples and pore dimension distribution (e); the pores are indicated with yellow arrows.

Figure 6. EDS spectra for: F₂ (a) and F₂20s (b) samples.

Figure 7. Porosity and density vs. temperature for all forsterite samples.

Figure 8. The effect of heat treatment on shrinkage and weight loss of all forsterite samples.

Figure 9. The compression strength of all forsterite samples.

Figure 10. SEM images magnification $\times 1000$ and $\times 20,000$ of F₁ (a,b) and F₁20s (c,d) samples, after 14 days in SBF (simulated body fluid).

Figure 11. SEM images magnification $\times 1000$ and $\times 20,000$ of F₂ (a,b) and F₂20s (c,d) samples, after 14 days in SBF.

Figure 12. EDS spectra for F₁, F₁20s samples (a) and F₂, F₂20s samples (b) after 14 days in SBF.

Figure 13. FTIR Spectra of F₁, F₁20s before and after 14 days in SBF.

Figure 14. FTIR Spectra of F₂, F₂20s before and after 14 days in SBF.

Figure 15. Florescence microscopy for images for F₁ (a), F₁20s (b), F₂ (c), F₂20s (d) and control (e) samples.

PART I - State of the Art

1. Introduction

The bone is one of the complex active metabolic organs [1-3], composed of cellular matrix and cells, which presents a complex, mineralized structure, whose main purpose is to provide to the body the support for its weight [1]. The cellular matrix is composed of collagen fibres, non-collagenous proteins, and inorganic minerals [1].

Bone handles important functions for the human body. The first one which is the most important is locomotion. Another function is to support and to protect soft tissues and bone marrow., and also, it's a significant storage of calcium (Ca) and phosphorus (P). It is a tissue of a connective nature, made up of two histologically distinct types: cortical bone tissue and trabecular bone tissue. It is made up of four main types of cells: bone lining cells, osteoblasts, osteocytes and osteoclasts [4].

Cortical bone tissue is found mainly in the diaphysis of long bones and has a primary role in support and protection. Trabecular bone tissue is found in the metaphysis and epiphysis of long bones, in short bones and in the diploe of broad bones, with a predominantly metabolic role given the large total surface area [5].

Bone is a composite material consisting of an organic and an inorganic phase. Depending on the mass, 60% of the bone tissue composition is inorganic matter, 8-10% is water, and the rest of the percentage is organic matter. By volume, inorganic matter represents 40%, water 25%, and organic matter 35%. The impure form of hydroxyapatite ($\text{Ca}_{10}(\text{PO}_4)_6(\text{OH})_2$) is the inorganic phase, which consists of calcium phosphate, while the organic phase is predominantly composed (by mass) of 98% collagen type I and of a variety of non-collagenous proteins (NCPs), and cells represent 2% of this phase.

The importance of bone replacement or regeneration becomes clear when it comes to the healing of fractures or cracks caused by an applied force or overuse [6], in the case of diseases such as osteoporosis and “osteogenesis imperfect”, in which normal bone formation and development are affected [7], but also in situations where the bone is removed via surgery due to trauma or infections that may occur at the bone level [8].

Due to their structural, chemical, physical properties, but also due to their mechanical properties, ceramics, metal alloys, polymers and composite materials are often utilized in biomedical applications. Both, ceramics and polymers can be used as biomaterials due to their biocompatibility, bioactivity and ability to bind bone, but also due to their flexibility and biodegradability. Bioceramics can be used in the field of orthopaedic and dental prostheses, and biopolymers can be used in the reconstruction and replacement of soft tissues and to obtain cardiovascular devices [33].

Calcium silicate ceramics have caught the interest of researcher interest since the mid-2000s to provide a suitable alternative for bone substitutes due to the issues encountered with clinically available ceramic composed of calcium phosphates and bioactive glasses. Also, these materials offer alternative solutions to cure bone tissue ailments, having great applicability in tissue engineering.

Biomaterials play a very important role in extending life and promoting its quality, because they could replace or repair diseases of organs, blood vessels or tissues. By definition, a biomaterial is any device, system, inert or active pharmacological substance, or a combination of these, with the purpose of implantation and incorporation into the biologically active environment to treat, improve and/or replace the function of affected tissues and organs [35].

There are three main categories of biomaterials in the design and fabrication of scaffolds, namely: ceramic [36], polymeric [37] and metallic [38]. The use of these materials independently, without using them to obtain composite materials, represents a limitation of

their properties. Thus, a solution in the case of limitations would be the use of composite scaffolds, formed from different phases. This approach is intuitive, because through the combination and complementarity of materials, optimal results can be obtained, which are closer to the standard of the human body.

PART II - Original contributions

General and specific objectives of the research

As a general objective of the research made within my PhD thesis is to come up with a certain contribution in the specialized literature that studies materials with the aim of integration into medical devices. This idea arose from the desire to develop new materials that can help doctors in their daily work and to help people who have problems with the skeletal system.

The main objective was to obtain porous scaffold type materials by modern methods for usage in bone reconstruction and regeneration. Bone reconstruction and regeneration and their need is clear in many cases where the normal bone development is affected. Osteoporosis, osteogenesis imperfecta and Paget's disease are three of the most well-known diseases of the bone system, being characterized by low bone density, fractures, and damage to the bone structure.

The proposed objective at the beginning of the study was focused on the calcium magnesium silicates and fibres synthesis as zero-dimensional (*0D*) structures, respectively one-dimensional (*1D*) structures as presented in *Fig. 34*. For obtaining the calcium magnesium silicates sol-gel method was used and for polymeric fibres the electrospinning method was used. Both processes are feasible for producing materials used in tissue engineering.

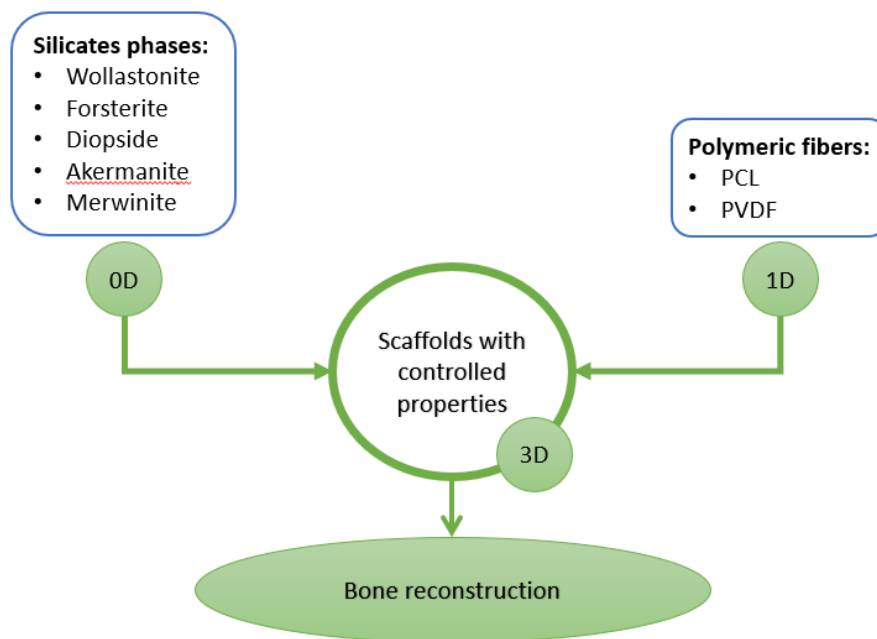


Fig. 34. The main materials obtained for the proposed objective.

The second objective was to make a complex characterization from a thermal, compositional, structural, morphological, mechanical, and biological point of view of the materials mentioned before. All the performed tests have the purpose of allowing the identification of the best materials and processing routes in order to obtain scaffolds with properties similar to natural bone.

The third objective was to obtain ceramic scaffolds based on calcium magnesium silicates and composite fibres loaded with mineral powders with different properties, such as bioactivity, biocompatibility, and good mechanical strength.

Another goal was to develop my career as a chemical engineer by disseminating the results in specialized journals and participating in conferences and meetings in the field of biomaterials.

General conclusions and originality

In biomedical field, various materials have been tested and used to obtain scaffolds for bone reconstruction. The perfect scaffolds must have bioactivity, biocompatibility, bioresorbability, but also to provide mechanical support for the entire human body.

During my PhD study, all the objectives proposed at the beginning were achieved and all the materials obtained and studied for their properties demonstrated potential for tissue engineering applications by bringing novelty in this biomedical field.

As it was mentioned before, this study was focused on the calcium magnesium silicates and polycaprolactone (PCL) and polyvinylidene fluoride (PVDF) fibres synthesis. Previously mentioned materials were synthesized by methods which are feasible for tissue engineering.

The current thesis was split in two parts: Part I – a review regarding the importance of calcium magnesium silicates, polymers type and fibres in tissue engineering and their main synthesis route used for obtaining composite materials based on polymeric fibres and mineral phases; Part II – an extended presentation of the original contribution and papers published in specialized journals.

Article 1 – Processing of Calcium Magnesium Silicates by the Sol–Gel Route. Gels - Q1, IF: 4.6

In *Article 1*, the calcium magnesium silicates were obtained by sol-gel method, which is known among the researchers for its simplicity and advantages, like excellent adherence during deposition for obtaining thin films and attaining morphological control, the uniform integration of the precursors, sintering at high temperatures of the obtained powders. In this paper, diopside, akermanite and merwinite powders were obtained by calcination at 600 °C and the characteristics for these ceramics were tested by thermal analysis, scanning electron microscopy (SEM), energy dispersive X-ray spectroscopy (EDX), Fourier transform infrared spectroscopy (FTIR), X-ray diffraction (XRD) and Rietveld refinement. As a conclusion, these ceramics sintered at different temperatures (800, 1000 and 1300 °C) have promising properties to make them desirable materials for tissue engineering.

The novelty of this paper consists in the comparative discussion of three types of silicate materials (diopside, akermanite and merwinite) obtained by the same method, sol-gel. Also, their sintering at different temperatures demonstrated the influence of increasing calcium content on crystallinity and morphological properties.

Article 2 – Composite Fibers Based on Polycaprolactone and Calcium Magnesium Silicate Powders for Tissue Engineering Applications. Polymers - Q1, IF: 5

In *Article 2*, PCL fibres were obtained by electrospinning method, followed by producing the composite PCL fibres with different content of inorganic powder. The composites were studied by EDX and FTIR, and the spectra showed the presence of embedded mineral entities. SEM analysis revealed a significant decrease in fibre diameter following loading, from 3 μm to less than 100 nm. It was also demonstrated that the bioactivity progressively grows from diopside, to akermanite and then to merwinite, with the Ca amount present in the composite material.

In this study, PCL fibres loaded with diopside, akermanite and merwinite were obtained for the first time in the specialized literature, more exactly, the combination of a bioactive material with a bioresorbable one. Because in this field there is limited research on such subject, their morphological and biological properties were also explored, and some influences from compositional and processing aspects were identified.

Article 3 – Comparative Study on TiO₂ Nanoparticles Obtained by Precipitation and Sol-Gel. U.P.B. Sci. Bull., Series B - IF: 0.5

In *Article 3* is presented a study were TiO₂ nanoparticles obtained by sol-gel method are compared with TiO₂ nanoparticles obtained by precipitation method starting from the same precursors and calcinated at 500 °C. It was demonstrated that the gel showed signs of a preliminary crystallization and after calcination presented both phases of TiO₂, anatase and lesser amount of rutile, while the calcined precipitate was a single-phase powder. It was also determined that in case of gel, the thermal analysis showed less/more weight loss steps and thermal processes than in case of precipitate. Also, the size of the particles in case of sol-gel route are smaller than in case if precipitation route, which means diameters below 10 nm.

The originality of this study is based on the comparison of the synthesis methods, with a focus on the effect they have on the final properties, by performing optical, structural, morphological, compositional, and thermal analysis on the dried intermediates, and also on the powders calcinated at 500 °C.

Article 4 – The Influence of Electrospinning Parameters on the Morphological Features of PVDF Fibres. Revista Română de Materiale / Romanian Journal of Materials - IF: 0.65

In *Article 4*, PVDF fibres were obtained by electrospinning method. The main purpose of this study was to assess different precursors to produce continuous and beadless fibres suitable for developing piezoelectric scaffolds. The electrospinning parameters, such as voltage, feeding rate and the distance between the spinneret and the collector were evaluated. The effect of polymer concentration and solvent used were studied too. Finally, our findings were that the ideal condition to obtain PVDF fibres is the one with 20 wt% polymer concentration, a 2:3 solvent ratio between dimethylformamide and acetone, 1 mL/h flow, 20 cm distance and 18 kV voltage. Moreover, to make these fibres more suitable for biomedical applications they were loaded with barium titanate to demonstrate their potential as piezoelectric composite.

This study brings in the scientific world the development of superior 1D structures by using different precursors and processing parameters. For the first time, such piezoelectric PVDF fibres were loaded with barium titanate nanoparticles in order to achieve piezoelectric binary composite.

Article 5 – Synthesis and Characterization of Porous Forsterite Ceramics with Prospective Tissue Engineering Applications. Materials - Q2, IF: 3.4

In *Article 5* the synthesis and characterisation of forsterite ceramics using sucrose as porogenic agent are presented. The forsterite ceramics were sintered at 1250 and 1320 °C in order to make a comparison of the results for all samples with or without sucrose by analysing XRD patterns, SEM images, EDS spectra, and measuring the porosity, density versus temperature. At the compressive strength tests, it was revealed that the most resistant sample was forsterite without porogenic agent sintered at 1250 °C, and it is suitable for replacing trabecular and cortical bones. The same analyses were also performed after immersion of the samples for 14 days in SBF and as expected, in SEM images was visible the HAp layer on the surface and by EDS was confirmed by presence of Ca and P, which are characteristics for apatite. The best cell viability was shown in case of forsterite ceramic sintered at 1320 °C with sucrose due to porous structure made by porogenic agent.

Article 5 presents forsterite ceramics as a potential material for bone tissue engineering by analysing their morphological and structural properties, as well as *in vitro* biocompatibility. Moreover, the novelty of this paper resides in the use of a porogenic agent, such as sucrose, to adjust the forsterite ceramics porosity.

All the published papers demonstrate the importance of calcium magnesium silicates and fibres in biomedical field. All the analysis were performed with the scope of demonstrating the best materials suitable for hard tissue reconstruction.

Results dissemination

First author publications:

1. **Alecu, A.-E.**; Costea, C.-C.; Surdu, V.-A.; Voicu, G.; Jinga, S.-I.; Busuioc, C. *Processing of Calcium Magnesium Silicates by the Sol–Gel Route*. Gels 2022, 8, 574.
Q1, IF: 4.6
2. **Alecu, A.-E.**; Balaceanu, G.-C.; Nicoara, A.I.; Neacsu, I.A.; Busuioc, C. *Synthesis and Characterization of Porous Forsterite Ceramics with Prospective Tissue Engineering Applications*. Materials 2022, 15, 6942.
Q2, IF: 3.4
3. **Alecu, A.-E.**; Girjoaba, S.-A.; Beregoi, M.; Jinga, S.-I.; Busuioc, C. *The Influence of Electrospinning Parameters on the Morphological Features of PVDF Fibres*. Revista Română de Materiale / Romanian Journal of Materials 2022, 52 (3), 1-10.
IF: 0.65
4. **Alecu, A.-E.**; Girjoaba, S.-A.; Enculescu, M.-M.; Busuioc, C. *Comparative Study on TiO₂ Nanoparticles Obtained by Precipitation and Sol-Gel*. U.P.B. Sci. Bull., Series B, Vol. 85, Iss. 1, 2023.
IF: 0.5
5. **Alecu, A.-E.**; Girjoaba, S.-A.; Beregoi, M.; Bacalum, M.; Raileanu, M.; Jinga, S.-I.; Busuioc, C. *Synthesis and Evaluation of Composite Scaffolds Based on PVDF Fibres and Mineral Powders for Medical Applications*. Revista Română de Materiale / Romanian Journal of Materials 2023, 53 (2), 150-160.
IF: 0.65

Co-author in publications related to the topic:

1. Busuioc, C.; **Alecu, A.-E.**; Costea, C.-C.; Beregoi, M.; Bacalum, M.; Raileanu, M.; Jinga, S.-I.; Deleanu, I.-M. *Composite Fibers Based on Polycaprolactone and Calcium Magnesium Silicate Powders for Tissue Engineering Applications*. Polymers 2022, 14, 4611.
Q1, IF: 5
2. Nicoara, A.I.; **Alecu, A.-E.**; Balaceanu, G.-C.; Puscasu, E.M.; Vasile, B.S.; Trusca, R. *Fabrication and Characterization of Porous Diopside/Akermanite*

Ceramics with Prospective Tissue Engineering Applications. Materials 2023, 16, 5548.

Q2, IF: 3.4

- Nicoara, A.I.; Voineagu, T.G.; **Alecu, A.-E.**; Vasile, B.S.; Maior, I.; Cojocaru, A.; Trusca, R.; Popescu, R.C. *Fabrication and Characterisation of Calcium Sulphate Hemihydrate Enhanced with Zn- or B-Doped Hydroxyapatite Nanoparticles for Hard Tissue Restoration*. Nanomaterials 2023, 13, 2219.

Q1, IF: 5.4

Conference attendance during PhD stage:

- RICCCE 2022, “22nd Romanian International Conference on Chemistry and Chemical Engineering”, *Electrospun Fibres Loaded with Active Powders as Multifunctional Hard Tissue Scaffolds*, September 2022, Sinaia, Romania.

Table 1. Cumulated impact factor

Journal	Impact Factor
Gels	4.6
Materials	3.4
Romanian Journal of Materials	0.65 + 0.65
UPB Scientific Bulletin	0.5
Polymers	5 (0.625)
Cumulated Impact Factor	10.425

Selective Bibliography

- J. An, S. Leeuwenburgh, J. Wolke, J. Jansen, *Mineralization Processes in Hard Tissue: Bone*, *Biominer. Biomater. Fundam. Appl.* 129–146, 2016.
- R. Florencio-Silva, G.R. da S. Sasso, E. Sasso-Cerri, M.J. Simões, P.S. Cerri, *Biology of Bone Tissue: Structure, Function, and Factors That Influence Bone Cells.*, *Biomed Res. Int.* 2015, 421746, 2015.
- E.F. Morgan, G.L. Barnes, T.A. Einhorn, *The Bone Organ System. Form and Function*, Fourth Edi, Elsevier, 2013.
- T. Bellido, L. Plotkin, A. Bruzzaniti, *Bone Cells*, *Basic and Applied Bone Biology*, Chapter 3, 37-55, 2019.
- J.J.B. Anderson, *OSTEOPOROSIS*, in: B.B.T.-E. of F.S. and N. (Second E. Caballero (Ed.), Academic Press, Oxford, 4278–4281, 2003.
- R. Marsell, T. A. Einhorn, *The biology of fracture healing*, *Injury*, 42(6), 551-555, 2011.
- J.O. Hollinger, A.O. Onikepe, J. MacKrell, T. Einhorn, G. Bradica, S. Lynch, C.E. Hart, *Accelerated fracture healing in the geriatric, osteoporotic rat with recombinant human platelet-derived growth factor-bb and an injectable beta-tricalcium phosphate/collagen matrix*. *J. Orthop. Res.*, 26: 83-90, 2008.
- F. J. Aragón-Sánchez, J. J. Cabrera-Galván, Y. Quintana-Marrero, M. J. Hernández-Herrero, J. L. Lázaro-Martínez, E. García-Morales, J. V. Beneit-Montesinos, D. G. Armstrong, *Outcomes of surgical treatment of diabetic foot osteomyelitis: a series of*

- 185 patients with histopathological confirmation of bone involvement.* Diabetologia **51**, 1962–1970, 2008.
33. S. Venkatraman, S. Swamiappan, Review on calcium- and magnesium-based silicates for bone tissue engineering applications, Journal of Biomedical Materials Research – Part A, 108(7), 1546-1562, 2020.
 35. S. V. Bhat, Overview of Biomaterials. Biomaterials, Chapter 1, 1–11, 2002.
 36. Y. No, J. Li, H. Zreiqat, Doped calcium silicate ceramics: A new class of candidates for synthetic bone substitutes, Materials, 10 (2), 2017.
 37. A. Nicolae, A. Grumezescu, Polymer fibers in biomedical engineering, Materials for Biomedical Engineering: Biopolymer Fibers, 1-20, 2019.
 38. L. Malladi, A. Mahapatro, A. Gomes, Fabrication of magnesium-based metallic scaffolds for bone tissue engineering, Materials Technology, 33(2), 173-182, 2018.